

# ECG Necklace: Low-power Wireless Necklace for Continuous ECG monitoring

Qiuyue (Shirley) Xue

Paul G. Allen School of Computer  
Science and Engineering  
University of Washington  
Seattle, Washington, USA  
qxue2@cs.washington.edu

Ruiqing Wang

Global Innovation Exchange  
University of Washington  
Seattle, Washington, USA  
ruiqing@uw.edu

Vikram Iyer

Paul G. Allen School of Computer  
Science and Engineering  
University of Washington  
Seattle, Washington, USA  
vsiyer@uw.edu

Eric Steven Martin

Department of Electrical & Computer  
Engineering  
University of Washington  
Seattle, Washington, USA  
esmartin@uw.edu

Antonio Glenn

Paul G. Allen School of Computer  
Science & Engineering  
University of Washington  
Seattle, Washington, USA  
aglenn5@cs.washington.edu

Jiaqing Liu

Department of Electrical & Computer  
Engineering  
University of Washington  
Seattle, Washington, USA  
jiaqing@uw.edu

Richard Li

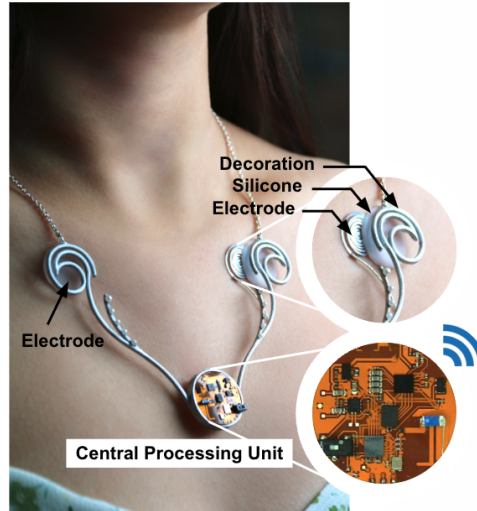
Paul G. Allen School of Computer  
Science & Engineering  
University of Washington  
Seattle, Washington, USA  
lichard@cs.washington.edu

Shwetak Patel

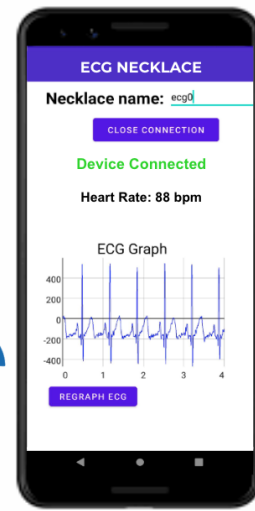
Paul G. Allen School of Computer  
Science & Engineering  
University of Washington  
Seattle, Washington, USA  
shwetak@cs.washington.edu



(a) ECG Necklace final form factor



(b) ECG Necklace exploded view



(c) ECG Necklace App

Figure 1: a) The ECG Necklace with fashion design. b) An exploded view of the ECG Necklace, showing the PCB beneath the central pendant and the novel skin moisture-enhanced electrodes. c) The smartphone app visualizing ECG data wirelessly transmitted from the necklace.

## Abstract

Continuous, everyday ECG monitoring is essential for detecting transient heart conditions and enabling early intervention in cardiovascular diseases. However, current technologies, such as ECG Holter monitors and smartwatches, face challenges in balancing continuous monitoring with long-term wearability due to trade-offs in electrode placement. To address this, we present a novel ECG



This work is licensed under a Creative Commons Attribution-NoDerivatives 4.0 International License.

CHI '25, Yokohama, Japan

© 2025 Copyright held by the owner/author(s).

ACM ISBN 979-8-4007-1394-1/25/04

<https://doi.org/10.1145/3706598.3713742>

necklace that leverages its natural placement on the chest to provide continuous, clinically valuable ECG monitoring. Our design positions two electrodes on the left and right sides of the chest, approximating standard Lead I placement for accurate cardiac diagnostics. The necklace features an innovative skin moisture-enhanced electrode design for sustained comfort and integrates a compact 22-mm processing unit as the pendant, offering a 4-day battery life. In our studies, the ECG necklace demonstrated performance comparable to FDA-approved Holter monitors, with key features falling within a timing error range of 3.2–15.7 ms—well within acceptable limits. In our in-the-wild study, participants rated the necklace as highly comfortable and preferred it over traditional ECG monitors. As a widely accepted everyday accessory, the ECG necklace has the potential to seamlessly combine advanced functionality with daily wearability.

## CCS Concepts

- Human-centered computing → Ubiquitous and mobile computing systems and tools; • Applied computing → Consumer health.

## Keywords

Wearable Computing; Health monitoring; ECG; Smart Jewelry;

### ACM Reference Format:

Qiuyue (Shirley) Xue, Eric Steven Martin, Jiaqing Liu, Ruiqing Wang, Antonio Glenn, Richard Li, Vikram Iyer, and Shwetak Patel. 2025. ECG Necklace: Low-power Wireless Necklace for Continuous ECG monitoring. In *CHI Conference on Human Factors in Computing Systems (CHI '25), April 26–May 01, 2025, Yokohama, Japan*. ACM, New York, NY, USA, 14 pages. <https://doi.org/10.1145/3706598.3713742>

## 1 Introduction

Cardiovascular diseases are the leading cause of death globally, accounting for an estimated 17.9 million lives or 32% of global deaths [62]. Electrocardiogram (ECG) is a key diagnostic tool in medicine to diagnose heart conditions. They record the electrical activity of a heart over a period of time using two or more electrodes placed on the skin. While widely used in clinics, ECG is difficult to schedule, and many heart conditions, such as arrhythmias, are transient, with symptoms that may disappear before diagnosis. In addition, 20% to 50% of heart attacks are “silent”, meaning patients experience no symptoms or unrelated symptoms, such as flu-like symptoms, instead of traditional symptoms like chest pain [10, 15, 52]. Without continuous ECG monitoring, these silent critical warning signs are unnoticed, and up to 50% of cases are diagnosed only after heart disease has progressed to a later stage [21].

Continuous, everyday ECG monitoring is critical for detecting the onset of heart diseases and enabling early intervention. However, achieving this in a daily wearable format remains challenging due to the trade-off between accurate electrode placement and wearability. Standard electrode placement, with electrodes far apart on different sides of the heart, is critical for accurate diagnosis but limits wearability. ECG Holter monitors use cumbersome cables to achieve standard placement but sacrifice comfort, making them suitable only for ambulatory monitoring. ECG patches improve wearability but rely on non-standard placements, limiting their

clinical utility to arrhythmia detection only. Consumer wearables like smartwatches, which use the left and right hand for electrode placement, cannot provide continuous monitoring. They require users to touch the watch crown to complete the circuit, allowing only brief 30-second recordings, which limits their suitability for continuous ECG tracking.

We address this challenge and provide continuous, clinically valuable ECG monitoring in a wearable format by leveraging the necklace’s natural shape around the chest. As shown in Figure 1, the necklace’s positioning allows two electrodes to be placed on the left and right sides of the heart, enabling similar to standard Lead I placement to capture horizontal heart activity for diagnosing a broad range of conditions. The ECG Necklace comprises a compact processing unit as the central pendant and two non-adhesive electrodes as adjacent pendants. In a study with 12 participants, we demonstrated that the necklace’s ECG signal is comparable to a Holter monitor with standard Lead I placement, providing a reliable signal for heart diagnostics. As necklaces are widely accepted as everyday accessories worn by millions, this form factor has the potential to become a consumer-friendly wearable for daily use.

Achieving continuous ECG sensing while ensuring long-term comfort presents significant challenges. Standard adhesive gel electrodes, while effective, are uncomfortable for extended wear due to skin irritation and are single-use only because of gel evaporation. To address this, we design a novel skin moisture-enhanced electrode that uses natural skin moisture as the electrode “gel” to improve the electrode performance. Since skin moisture (i.e., sweat) is deformable and conductive due to electrolytes, it improves the skin contact with the metal electrode and improves the signal quality [3, 30], like traditional ECG gels. As human skin continuously produces moisture that evaporates into the air [1], we leveraged a thin layer of skin-friendly silicone that acts as a barrier against water evaporation from the skin, creating a moisturizing micro-environment as “gel” for the electrode. Unlike adhesive electrodes, the skin-friendly necklace electrodes avoid skin irritation and do not suffer from gel evaporation by leveraging the continuous production of moisture by the body.

In addition to electrode comfort, developing a wireless smart necklace requires addressing several technical challenges related to size, weight, and battery life to ensure long-term wearability. Size constraints directly affect power consumption due to the limited energy density of batteries. To design a wireless system within these limitations, we utilized a highly integrated ECG analog front-end chip and an ultra-compact nRF52 microcontroller. By carefully optimizing both size and power consumption, we achieved a compact design with a 22 mm, 4-gram pendant—over four times smaller than the smallest continuous ECG patches [6, 59, 69]. The ECG necklace offers a 4-day battery life with continuous 250 Hz sampling and wireless streaming, which can be further extended by reducing the sampling rate.

We investigated various aspects of the ECG necklace design, including electrode placement, electrode design, and the necklace’s overall performance in natural daily scenarios. We evaluate the novel electrode design by a benchmark test and a twelve users experiment, showing that our electrode with diameters between 15–25 mm achieve impedance and Signal-to-Noise Ratio (SNR) comparable to those of the standard adhesive gel electrodes. We compare

the ECG Necklace's performance versus an FDA-approved Holter monitor in real-world testing, with twelve participants performing common activities (talking, using laptops and smartphones). We validated the difference between the key features from the ECG necklace and Holter monitor is only 3.2 ms for the R peak, 8.5 ms for the P peak, and 15.7 ms for the T peak, all of which are well within the generally acceptable error range of 20 ms [14]. In addition, we conducted a whole-day in-the-wild study with ten users wearing the necklace and a consumer heart rate chest strap with ECG sensing. The ECG Necklace demonstrates comparable ECG signal availability to the tightly worn chest strap and 1.5 dB higher signal quality than the chest strap. In addition, nine out of ten users strongly prefer the necklace over the commercial chest strap in terms of comfort, indicating its potential as a daily ECG and health monitoring system.

We summarize this paper's **contributions** below:

- We developed a wireless necklace for continuous ECG monitoring by utilizing the necklace's unique shape for accurate electrode placement while maintaining wearability. The ECG necklace features a compact design with a 22-millimeter diameter pendant with an 88-hour-long battery life.
- We designed a novel skin-moisture-based electrode using silver PCB and silicone. We conducted a benchmark test and an on-user experiment to characterize the electrode's size, frequency response, impedance at different moisture levels, and actual on-user performance.
- We conducted real-world studies to assess the ECG Necklace's signal quality compared to an FDA-approved ECG monitor. We further conducted a whole-day in-the-wild study to evaluate the ECG Necklace's signal availability, quality, and comfort level in natural daily settings compared to a commercial chest strap.

## 2 Related Work

### 2.1 Smart Jewelry

Smart jewelry is an emerging class of wearable devices that seeks to combine fashion and function by integrating sensing into jewelry accessories. Previous work exploring smart jewelry items include smart necklaces, which have been used for silent speech recognition [68] and medication adherence detection [29], bracelets for user interaction [25, 56], health monitoring and intervention [2, 24], rings for interaction [4] and health monitoring [71], and earrings for wellness tracking [27, 47, 64]. None of these have demonstrated continuous ECG. By integrating various sensors and communication technologies, smart jewelry enables a variety of applications for health sensing, user interaction, and information sharing.

### 2.2 ECG Monitor

There have been numerous research efforts to make ECG sensing more accessible to common people in daily life. Figure 2 summarizes the main efforts, including ECG holter monitors, patch monitors, chest straps, smartwatches, and efforts in the research field. ECG Holter monitors are usually for extended ambulatory monitoring featuring hand-size devices with cables connected to adhesive electrodes [13, 20]. While the long cables enable standard electrode

	Holter monitor	ECG patch	Chest strap	Smart watch	2011 necklace	Our Work
<b>Everyday wearing</b>	No, ambulatory monitoring only	No, ambulatory monitoring only	No, typically only during exercise	General wearable for everyday use	No, ambulatory monitoring only	General wearable for everyday use
<b>Continuous</b>	Yes	Yes	Yes	Not continuous	Yes	Yes
<b>Electrode connection</b>	Connect to device through cables	Electrodes are within device	Electrodes are within device	Electrodes are within device	Connect to device through cables	Electrodes are within device
<b>Electrode placement</b>	Standard clinical placement	Non standard, only for arrhythmia	Non standard, only for heart rate	Standard Lead I placement	Standard Lead II placement	Standard Lead I approximate
<b>Electrode type</b>	Adhesive	Adhesive	Non adhesive	Non adhesive	Adhesive	Non adhesive
<b>Size and weight</b>	~110x70x30mm ~100 grams	90x28x8mm ~ 15 grams	~65x34x10mm ~ 60 grams	~ 44x44x12mm ~ 40 grams	60x40x10mm 20 grams	22x22x4mm, 5 grams

**Figure 2: A comparison table of existing ECG monitors and our work.**

placement, they also make the device cumbersome to use and restrict user movements. As a result, these devices have never gained traction outside of clinical use. More recently, there are patch-like ECG Holter monitors with adhesive electrodes [45, 59, 70]. These patches are prescribed by clinicians for extended ambulatory monitoring. However, their non-standard electrode placement, limited by the patch's contact area, restricts their use to arrhythmia detection (e.g., AFib) only rather than full ECG diagnostics.

Commercial products such as chest straps and smartwatches have integrated ECG measurement too. Polar H10 and Frontier X2 are chest straps designed for heart rate monitoring during exercise [26, 48]. The ECG sensing is only used for monitoring heart rate instead of any diagnosis because of its non-standard electrode placement. Commercial smartwatches or KardiaMobile also support ECG measurement by putting the finger from another hand on the crown of the smartwatch, but they cannot support continuous ECG monitoring [3, 23, 30].

Researchers have explored continuous ECG monitoring from various wearables such as necklaces and earbuds. In 2011, Penderson et al. presented an ECG Necklace with adhesive electrodes for sensing ECG [46]. However, as seen in Figure 2, their design uses adhesive electrodes placed on the upper right and lower left of the chest, far outside the perimeter of the necklace form factor. This design ultimately resembles a Holter monitor more than a compact necklace. In addition, the central pendent of the system is 10 mm in height, making it easy to see under clothing and limiting its practicality and social acceptability for daily wear. Besides the necklace form factor, researchers have also explored using the earbud form factor for ECG sensing and R-peak detection [18]. Moreover, Bhattacharya et al. proposed a wireless electro-mechanical E-Tattoo for ECG and Ballistocardiogram (BCG) sensing, which leverages an adhesive layer to stick to the skin [7]. Researchers have explored reconstructing ECG signals from heart vibrations [9, 44] and UWB [61]. Vibcardiogram estimated ECG from wrist-worn wearable [9]. HeartQuake estimated ECG patterns from geophone-based sensing on a bed mattress [44].

### 2.3 Dry Electrode

Traditional adhesive gel electrodes, despite providing high-quality ECG signals, are unsuitable for long-term monitoring due to gel evaporation and skin irritation. Researchers have been developing gel-free dry electrodes for long-term ECG monitoring.

Smartwatches and Kardia mobile devices measure ECG signals when a finger is placed on the crown, leveraging the natural moisture of the finger—one of the most hydrated parts of the body—to enable effective sensing with dry electrodes [3, 23, 30]. Beyond leveraging finger moisture, the Frontier device employs chest strap pressure to increase the electrode-skin contact[26], although this pressure may affect comfort for some users.

Kim et al. present a detailed overview of research on soft and dry electrodes, identifying key characteristics — high conductivity, strong adhesion, stretchable, and biocompatible essential for high-performance dry electrodes[32]. Material scientists have explored various conductive materials for dry electrodes, including metals, conductive carbon-based materials such as graphene [35, 55] and carbon-nanotube [37], and conductive polymers such as PE-DOT:PSS [19, 38] and polypyrrole (PPy) [66]. Beyond different materials, researchers also have explored different methods for adhesion to the skin[39], including gecko-inspired microstructures[33] and octopus-like patterned structure [11, 12] to achieve adhesion through van der Waals force. To enhance skin-electrode contact and reduce the impedance mismatch, researchers have explored materials modification and micro-structure modification, including altering Young's modulus [67], bending stiffness [36], and innovating structural designs like ultra-thin films and tattoos [22, 28, 42].

### 3 Background on ECG

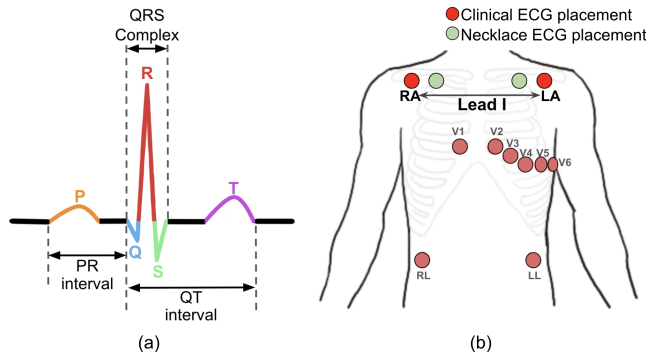


**Figure 3:** (a) Example of an ECG waveform from a heart in normal sinus rhythm. (b) The electrode placement in clinical standard 12-Lead ECG and the necklace's electrode placement.

ECG operates by detecting small electrical voltages generated by the depolarization and repolarization of the heart muscles during each cardiac cycle. ECG can be measured by placing a pair of ECG electrodes at two locations on the body and recording the voltage difference between them. Each pair of electrodes forms a lead and represents the axis along which the cardiac vector is visualized.

The typical ECG waveform, as shown in Figure 3, consists of three primary elements: the P wave, the QRS complex, and the T wave, each corresponding to a different part of the heart. Medical professionals analyze the ECG by examining the waveform's overall shape, timing and magnitude of the P, QRS, and T wave. Variations in these parameters can reveal a wide array of cardiac conditions. For example, atrial fibrillations (AFib) is diagnosed by looking for the absence of regular P waves and the presence of irregular R-R intervals.

### 3.1 Electrode Placement Requirement

Electrode placements have to follow standard guidelines, which clinicians heavily rely on for accurate diagnosis [31, 49]. Figure 3 (b) shows the standard 12-lead ECG setup utilizing 10 electrodes. They can be simplified by choosing just the RA, LA, and LL electrodes to form a 3-lead or 1-lead ECG. Lead I setup is one of the most common setups, with the negative electrode (RA) positioned on the right shoulder below the right clavicle and the positive electrode (LA) positioned on the left shoulder. Lead I captures the heart's electrical activity along the horizontal axis and provides insight into a wide range of heart conditions, making it suitable for the ECG necklace setup. We will discuss and evaluate electrode placement in the ECG necklace in Section 4.3.

### 3.2 Electrode Design

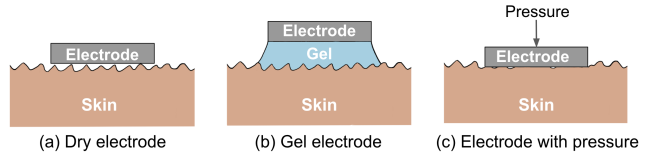


**Figure 4:** Demonstration of skin contact with (a) a simple dry electrode, (b) a gel electrode, (c) a dry electrode when pressed to the skin

ECG electrodes are essential parts for obtaining accurate ECG signals. These electrodes, typically made from conductive metals, are attached to the skin to transmit voltage signals from the body to the ECG device. The most common electrodes are adhesive gel electrodes that adhere tightly to the skin, with a layer of conductive gel between the skin and the electrode to enhance ECG voltage signal transmission. The necessity for conductive gel arises from the skin's uneven textures on a micro-level, which limits the amount of contact surface between the skin and the electrode.

As shown in Figure 4 (a), without conductive gel, the contact surface area between skin and electrode is minimal. The resulting air gap between the skin and electrode acts as an insulator to voltage, ultimately reducing the quality of the obtained signal. In comparison, conductive gel bridges the skin-electrode gap as shown in Figure 4 (b), which not only significantly increases skin-electrode surface contact but also improves the impedance mismatch between the human body and the electrode. Although adhesive gel electrodes ensure a high-quality ECG signal, they are uncomfortable to wear for extended periods, and the residue from the adhesive layer can remain on the skin for multiple days. Additionally, the electrodes stop working once the gel evaporates, typically within two hours of air exposure.

Besides adhesive gel electrodes, applying increased pressure on the electrode towards the skin can also enhance skin-electrode contact, as demonstrated in Figure 4 (c). Devices such as chest strap-based ECG and smartwatches use elastic bands to apply this pressure and improve signal quality. However, excessive pressure can be uncomfortable for users and unsuitable for devices like necklaces.

## 4 System Design

Designing a smart necklace wearable device requires a careful balance between functionality, user comfort, and aesthetic appeal. In this section, we will introduce the key components of the ECG necklace system. As shown in Figure 5 These include the ECG sensing front-end chip, the innovative design and strategic placement of ECG electrodes, an accelerometer for motion tracking, wireless communication technology for seamless data syncing, and the battery that powers the entire system. We will discuss how each element has been thoughtfully selected and integrated to optimize both performance and design aesthetics.

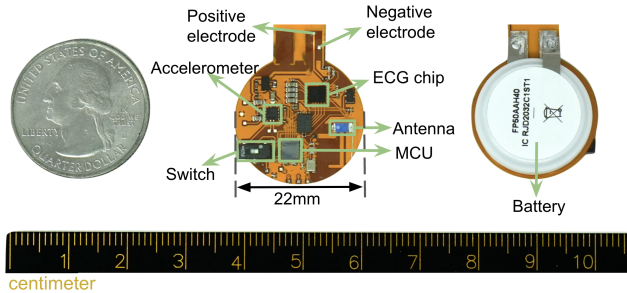


**Figure 5:** The front and back sides of the ECG necklace system, with a US coin as reference for size.

### 4.1 ECG Analog Front End

We implemented the ECG sensing analog front end using the MAX30003 chip, which features a compact size of 2.3 mm by 2.8 mm and ultra-low-power consumption of 100  $\mu$ A. To maximize the quality of ECG readings, the MAX30003 was set to operate at its highest amplification gain setting of 160 V/V and a sampling frequency of 250 Hz. The communication between the chip and the system's microcontroller is established through an SPI communication interface. ECG data captured by the MAX30003 is temporarily stored in a FIFO buffer, capable of holding up to 32 samples. This configuration allows the microcontroller to retrieve data from the buffer every 64 milliseconds, ensuring timely processing of ECG samples while reducing the frequency of microcontroller wake-ups to conserve power.

### 4.2 Dry Electrode

As discussed in Section 3.2, acquiring a high-quality ECG signal typically requires the use of either conductive gel, sufficient pressure, or adhesion to ensure the electrode's contact with the skin without any air gaps. However, excessive pressure and strong adhesion are not suitable for long-term comfort.

To address these challenges, we have developed an innovative solution: a flexible silver-based electrode with a flexible silicone film layer as its substrate. This design leverages the flexibility of the silicone layer to not only secure the electrode against the skin but also to create a moisturizing micro-environment between the skin and the electrode. Given that human skin naturally loses moisture through transepidermal water loss (TEWL), where the silicone layer acts as a barrier against water evaporation, ensuring a moist interface. Additionally, the natural conductivity of human sweat,

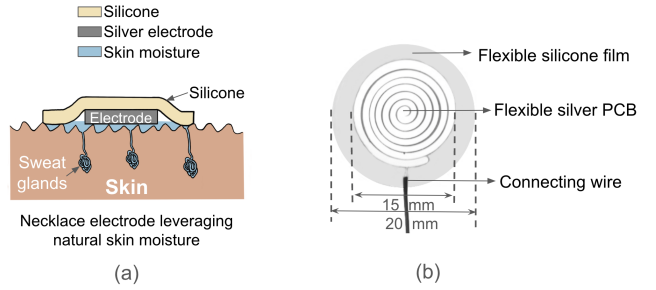


**Figure 6:** (a) The demonstration of the necklace electrode that leverages natural human skin moisture as the ECG "gel". (b) The components of the necklace electrode.

because of electrolytes such as sodium, chloride, potassium, and magnesium, facilitates its role as a conductive gel in this setup. Silicone was chosen because of its skin-friendliness. It is biocompatible, hypoallergenic, and does not promote bacterial growth, making it widely used in a range of skincare and medical applications, including being a gold standard for non-invasive scar treatment [60]. Silicone patches occlude and hydrate the stratum corneum of the treated skin area. After applying the silicone patch, the rate of water loss via evaporation of the treated skin area is much less than the untreated area, making the skin adequate but not over-hydrated [54]. Furthermore, the design is enhanced by the electrode pendant's weight, which applies a gentle and comfortable pressure to augment skin contact without compromising comfort.

Figure 6 shows the structure of our designed electrode. The conductive layer is a silver-coated flexible PCB, which can be fabricated through the standard process. This PCB, with a diameter of 15 mm and a thickness of 0.1 mm, is coated with silver to ensure optimal conductivity [32]. Its flexibility is further augmented by a laser-cut swirl pattern, enabling it to conform to the skin's texture. A thin wire is soldered to the silver-coated flexible PCB to connect the electrode with the necklace's central system. As any wire on the skin side of the flexible PCB could significantly increase the air gap between the skin and the electrode, we utilized vias on the PCB to connect the front side and the back side of the PCB, and the wire is soldered on the back side of the PCB to avoid causing air gap. The silicone layer is produced using Smooth-On EcoFlex 00-10, a user-friendly pourable silicone. Inspired by silicone scar patch and silicone wrinkle patch, we mixed the silicone base liquid, its curing agent, and simple body lotion in a 1:1:1 ratio. By curing it at room temperature, a highly flexible and stretchable silicone rubber is formed. The addition of lotion makes the silicone patch slightly adhesive without the need for glue, enhancing its ability to adhere to the skin without causing irritation. Our innovative necklace electrode is easy to manufacture yet effective. We will evaluate the performance of the electrode in Section 6.2.

### 4.3 Electrode Placement Design Space

We explore the necklace's unique design space by testing five different electrode placements to achieve a balance between clinical value and aesthetic appeal. Figure 7 illustrates the electrode placements we tested and the corresponding example ECG signals obtained from each configuration.

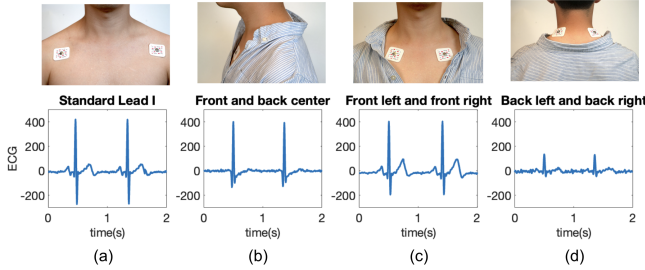


**Figure 7: ECG signals from different electrodes placement:** (a) standard clinical lead I placement, (b) front center and back center, (c) front left and front right under the collarbones, (d) back left and back right.

**Standard Lead I configuration:** Figure 7 (a) shows the electrode placement and its corresponding signal from Lead I configuration. It clearly contains the P wave, QRS complex, and T wave, and we will use it as the reference for the electrode placement experiment.

**Front center and back center:** Figure 7 (b) shows the placement and data from the front center and back center. This placement is particularly convenient for concealing the technology within the necklace, with the electrodes hidden behind the central pendant. As shown in Figure 7 (b), ECG signals obtained from this placement showed clear QRS complex but almost no P wave, which is important for many heart conditions diagnosis such as AFib and heart attack. Despite its limited clinical value, this setup can still provide valid heart rate and arrhythmia monitoring and detect Ventricular Hypertrophy from a widened QRS complex, which is worth exploring in the future.

**Front left and front right:** Figure 7 (c) shows the placement and data from front left and front right. The electrodes were placed at the extended line of the neck and below the clavicle. Given that the width of an adult's heart is approximately 8 cm (3.5 inches)—about the size of a person's fist [16]—and typically narrower than the neck width. This placement strategy allows for capturing the heart's ECG signal on the horizontal axis, and its signal shows valid P wave, QRS complex, and T wave, with almost the same shape as the standard lead I placement, with the potential to provide highly valuable clinical data.

**Back left and back right:** Figure 7 (d) shows the back left and back right electrode placement and corresponding signal. This electrode setup captures the heart's activity from a similar horizontal angle as those on the front, yet they have a much higher noise level, likely due to more attenuation.

In addition to the electrode placements shown in Figure 7, we have also tested the electrode placements combining the front center with either the back left or back right. However, this electrode placement does not show consistent ECG waveforms across different users, which is likely due to these configurations capturing only half of the heart's electrical activity, leading to distorted and variable ECG waveforms. So we do not recommend these electrode placements, and they are not included in Figure 7.

**Design choice:** We chose the electrode placement on the front left and right for our final design, considering its high SNR and similarity to standard Lead I configuration. However, there is a trade-off between aesthetic appeal and clinical value. While some

electrode configurations may capture only partial ECG data, they are still valuable to explore in the future.

#### 4.4 Other Sensing Capabilities

Though this paper mainly focuses on the ECG sensing part, we envision the necklace has the potential to become a daily health and fitness tracker. Thus, we have integrated motion sensing capability to it. We selected the LIS2DW12 accelerometer to sense the user's movements. It features a low active current consumption of 1 uA and a sensitivity of 0.244 mg/digit, which offers configurable settings for both the sensing scale and sampling rate. The accelerometer is set to sample at 50 Hz, which is high enough to track human motions. This addition can potentially turn the necklace into a comprehensive health monitoring platform capable of tracking physical activity, breathing patterns, and subtle seismocardiography (SCG) signals. However, since the accelerometer signal analysis on the chest is well studied [9, 44], this work does not focus on analyzing the accelerometer data.

#### 4.5 Bluetooth Communication and MCU

The ECG necklace is designed to be fully wireless, prioritizing comfort and ease of use. Bluetooth Low Energy (BLE) was chosen for its low power consumption, sufficient range, and reliable data transfer rates, making it ideal for this application. The nRF52832 microcontroller was chosen to implement BLE data streaming and interfacing with the sensors. It features a compact size (3.0 x 3.2 mm) and energy efficiency, which are essential for the compact design of the ECG necklace. To conserve energy, the microcontroller operates primarily in deep sleep mode, waking briefly for data exchanges and BLE transmission.

Every 120 milliseconds, the nRF microcontroller retrieves data from the FIFO buffers of the MAX30003 ECG chip and the LIS2DW12 accelerometer chip. This interval matches the ECG chip's capacity to store up to 32 samples, preventing data loss. During each wake cycle, the microcontroller reads 30 ECG samples and 18 accelerometer samples (6 from each axis), packages them into a single transmission packet, and sends it via Bluetooth before returning to deep sleep. This efficient process minimizes active time, maximizing battery life while enabling continuous, real-time monitoring.

#### 4.6 Battery

We selected the RJD2032C1ST1 rechargeable battery to power the entire ECG necklace system. This battery offers an 87 mAh capacity and features a compact, round form factor with a diameter of 20 mm and a thickness of 3.5 mm. While certain hearing aid batteries of a similar size offer higher capacities, they cannot be recharged due to their chemical compositions.

#### 4.7 The Final Necklace Design

Figure 8 shows the final necklace design and how a user would wear it. The pendant contains the main necklace system and is made on a round, flexible Printed Circuit Board (PCB). The front side of the PCB houses all the electronics, including the ECG front-end chip, Bluetooth microcontroller, and an accelerometer for potential motion sensing. The positive and negative electrodes for ECG sensing are wired to this side of the PCB. Meanwhile, the back side of the



**Figure 8: Demonstration of wearing the ECG Necklace (without any fashion decorations).**

PCB is dedicated exclusively to the battery. This double-sided PCB design maximizes the use of the limited area while maintaining a slim and wearable profile. The battery life is 88 hours, supporting continuous ECG signal streaming at 250 Hz and accelerometer signal streaming via Bluetooth. Besides the pendant, the two electrodes are placed under the collarbone, with a thin piece of silicone to hold it onto the skin. The entire necklace system weighs approximately 5 grams, with the central pendant (including the battery) weighing 4 grams and the two silicone-covered electrodes weighing 1 gram. Additionally, fashion components can be added to the necklace to enhance its aesthetic appeal and social acceptance. With the 3D-printed fashion design cover shown in Figure 1, the necklace has a total weight of 7 grams. We further discuss adding fashion components to the necklace in Section 9.1.

## 5 Signal Processing Pipeline

In this section, we present the signal processing pipeline for the ECG data and define the evaluation metrics for later sections.

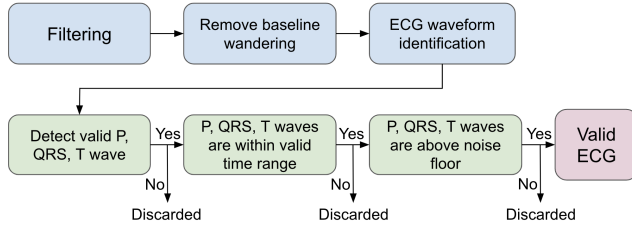


**Figure 9: The processing pipeline for ECG data.**

**Filtering:** Indoor environments contain significant electrical interference, primarily from 60 Hz or 50 Hz powerline signals coupled to the human body. To address this issue, we designed a band-stop filter targeted specifically at 60 Hz or 50 Hz—depending on the country’s powerline standard—as well as its harmonics at 120 Hz or 100 Hz. The filter has a narrow 2 Hz stopping bandwidth to minimize impact on other frequencies.

**Remove baseline wandering:** Baseline wander is a common low-frequency artifact in ECG recordings caused by movements and breathing. To address this, we used a wavelet decomposition-based method proposed by Sargolzaei et al. [51], now widely used

in ECG processing. This method analyzes the power of the baseline relative to the ECG signal through continuous signal decomposition. Unlike high-pass filters that require fine-tuned parameters and risk introducing artifacts, the wavelet-based approach is automatic and parameter-free, ensuring effective artifact removal.

**ECG waveform identification:** After removing noise and motion artifacts from the ECG signal, we identify the P, R, and T waves in the ECG signals using a popular open-source Python library NeuroKit2 [40]. These identified peak results are later used to assess the validity of the ECG waveform and its signal-to-noise ratio (SNR). It should be noted that ECG is a complex signal containing three main peaks but with various shapes. Even the highest accuracy processing method can still generate errors. NeuroKit2 yields the best detecting accuracy among the other toolkits we tested, thus it is chosen for our final signal processing pipeline.

**Valid ECG identification:** We used the detected P, R, T wave from NeuoroKit2 to classify whether the signal is a valid ECG. We define a valid ECG as:

1) the NeuroKit2 tool can successfully detect valid P waves, R waves, and T waves instead of returning NaN.

2) The identified P wave, R wave, and T wave are within a reasonable time interval range. Specifically, the interval between P peak and R peak should be in 50 to 200 milliseconds range [50], and the interval between the R peak and T peak should be in 200 to 400 milliseconds range [50].

3) The identified P wave, R wave, and T wave’s amplitude is higher than the noise floor in the heartbeat cycle. The noise signal is defined as the signals between two adjacent heartbeat cycles.

**Signal to Noise Ratio (SNR):** We use the detected P, R, and T wave’s amplitude and timing information to compute the SNR of the ECG signal. There have been different definitions of SNR for ECG signals, in this work, we use the traditional SNR definition that has also been used by many previous works:  $SNR = \frac{P(signal)}{P(noise)} = \frac{A^2(signal)}{A^2(noise)}$ . In the evaluation section, we reported the SNR in decibels, which is  $SNR_{db} = 10\log_{10}SNR$ . The signal amplitude  $A(signal)$  is the peak value of the P, R, or T wave, while the noise amplitude  $A(noise)$  is derived from signals between two heartbeats. The noise segment starts 350 ms after the R peak (end of the T wave for most healthy adults [50]) and ends 200 ms before the next R peak (before the P wave [50]). Although the noise segment ideally spans from the end of the T wave to the start of the next P wave, detecting these boundaries robustly is challenging. Tools like NeuroKit2 can introduce errors, even with ground-truth data. Thus, we use this timing-based segmentation as a practical proxy for assessing ECG signal quality.

## 6 Electrode Evaluation

We conducted a benchmark test and an on-user experiment to evaluate our novel electrode, with a diameter ranging from 25 mm to 5 mm, as shown in Figure 10. Larger electrodes, providing greater skin contact area, typically result in better signal quality. This variation in size helps us explore the limitations of dry electrodes and identify the optimal balance between signal quality and electrode size. All the studies in this paper have received Institutional Review Board (IRB) approval, and participants were compensated based on their involvement in the different studies.

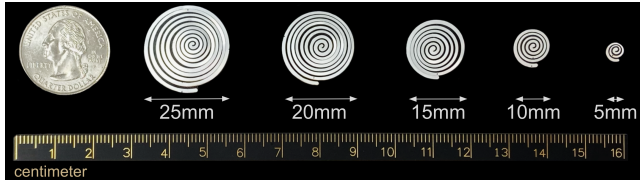


**Figure 10:** Tested necklace electrodes with diameters ranging from 25 mm to 5 mm.

## 6.1 Electrode Benchmark Test

We conducted benchmark tests to evaluate our electrode's frequency response in comparison to standard adhesive electrodes, as well as to assess how its impedance varies with different moisture levels.

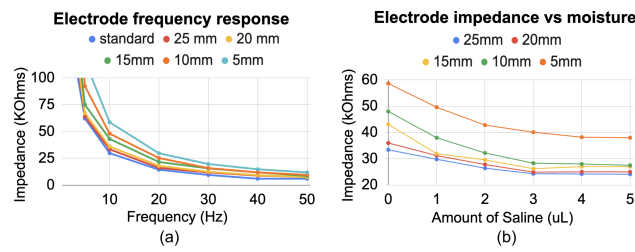


**Figure 11:** (a) The impedance of our electrodes (without moisture) and the standard adhesive electrode at different frequencies. (b) The impedance of our electrode at 10 Hz with different amounts of moisture level.

**6.1.1 Electrode Frequency Response.** Skin-electrode impedance is a key metric for evaluating an electrode's performance, as it reflects how effectively the ECG signal is transmitted from the body to the electrode. Lower impedance indicates better signal quality, with reliable ECG measurements typically requiring impedance below  $50\text{k}\Omega$  at 10 Hz, and values under  $10\text{k}\Omega$  being optimal [43].

We measured the skin-electrode impedance with diameters ranging from 5 mm to 25 mm, as well as a standard adhesive electrode, across different frequencies. The impedance was determined using a standard measurement circuit that computes voltage drop and current through the skin-electrode interface [5, 53, 57]. Since ECG signals predominantly span 1–100 Hz, with most power concentrated in the 1–50 Hz range [63], we focused on this frequency range. Figure 11 (a) shows that skin-electrode impedance decreases with increasing frequency, consistent with existing studies [5, 57, 65]. The standard gel electrode (3M Red Dot electrode) was measured as  $169\text{k}\Omega$  at 1 Hz,  $29\text{k}\Omega$  at 10 Hz, and  $6\text{k}\Omega$  at 50 Hz. Among our designs, the 25 mm electrode had the lowest impedance, measuring  $203\text{k}\Omega$  at 1 Hz,  $33.4\text{k}\Omega$  at 10 Hz, and  $7.5\text{k}\Omega$  at 50 Hz. In contrast, the 5 mm diameter electrode, due to its smaller contact area, exhibited the highest impedance:  $502\text{k}\Omega$  at 1 Hz,  $58.7\text{k}\Omega$  at 10 Hz, and  $12\text{k}\Omega$  at 50 Hz. While the 25mm, 20mm, and 15mm all demonstrated impedance below  $50\text{k}\Omega$  at 10 Hz, their values are higher than the standard adhesive electrode. However, this can be compensated by the body moisture, as demonstrated in the later experiment. In addition, it should be noted that these tests were conducted without skin preparation to simulate everyday usage scenarios. While

this results in higher impedance compared to ideal conditions, the findings align well with previous studies [8, 57, 58].

**6.1.2 Electrode Impedance Versus Moisture Amount.** We further investigated the effect of moisture on skin-electrode impedance by applying different amounts of saline to the skin using a pipette to simulate body moisture. Figure 11 (b) demonstrates how skin-electrode impedance at 10 Hz changes with the amount of saline added. All electrodes demonstrated a clear reduction in impedance with increased moisture. Specifically, the 15 mm, 20 mm, and 25 mm electrodes achieved impedance values comparable to standard adhesive electrodes with just  $2\mu\text{L}$  of saline, while the 10 mm electrodes required  $3\mu\text{L}$  to reach similar values. The impedance of the 5 mm electrode also decreased but did not match the performance of the larger electrodes, likely due to its limited contact area. The impedance of all electrodes converged with saline amounts exceeding  $4\mu\text{L}$ . On average, adults sweat approximately  $105\text{g/m}^2/\text{h}$  at the front chest during rest and  $248\text{g/m}^2/\text{h}$  during exercise [17]. For a 20 mm diameter electrode, this corresponds to a sweat production of  $105\text{g/m}^2/\text{h} \times (\pi \times (0.01\text{m})^2) = 0.033\text{g/h} = 0.55\text{mg/min}$  during rest. Assuming a saline/sweat density of  $1\text{mg}/\mu\text{L}$ , it would take about 6 minutes to generate  $3\mu\text{L}$  of moisture under ideal conditions. However, in real-world scenarios, this process may take longer since the silicone cover can reduce moisture evaporation but does not completely stop it [54].

## 6.2 Electrode Performance Evaluation

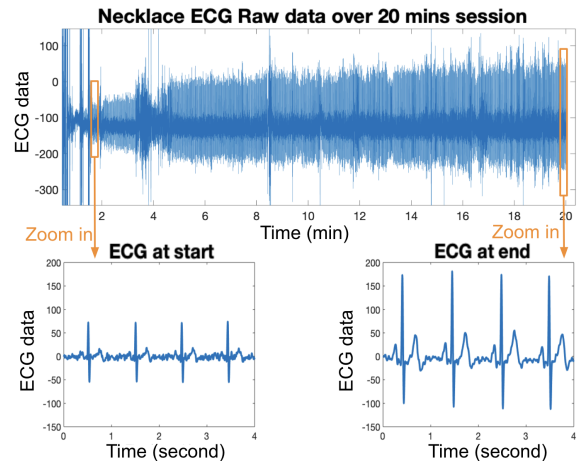


**Figure 12:** Example of an ECG signal obtained from the necklace electrode over a 20-minute period, with the zoomed-in plots on the signal at the start and at the end.

We evaluated our necklace electrode's performance over time with varying electrode sizes. For this evaluation, twelve participants were recruited (eight females, four males, average age  $28.2 \pm 4.8$ , average BMI  $21.9 \pm 2.2$ ), each of whom wore five necklaces with different electrode sizes. The sequence in which the necklaces were worn was determined using a modified balanced Latin square order to eliminate any effects from the order of testing. Participants were instructed to wear each necklace for 20 minutes while engaging in their typical daily activities, such as working on a computer while

seated. In addition, participants were asked to remain relatively still for at least 30 seconds every three minutes, allowing us to obtain reliable spot-check ECG readings free from motion artifacts. Besides testing the necklace electrode with various diameters, we also collected ECG signals using a standard adhesive gel electrode for one minute, which serves as a reference.

As discussed in Section 4.2, our necklace electrode uses a silicone layer to retain natural skin moisture, acting as a conductive gel to enhance signal quality. Since human skin continuously produces moisture, the ECG signal improves over time. Figure 12 shows an example from a 20-minute session. Initially noisy, with an SNR of 23 dB, the signal improved to 32 dB by the end. The SNR increased rapidly in the first few minutes as moisture filled the gap between the electrode and skin, then stabilized or improved gradually upon reaching an optimal moisture level. Similar patterns were observed in all participants, though the time to reach saturation varied between individuals.

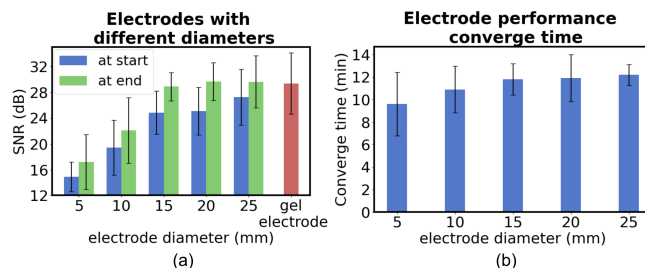


**Figure 13:** (a) The average ECG SNR obtained from electrodes with different diameters. (b) The average ECG signal quality converging time.

Figure 13 (a) shows the aggregated users' QRS peak SNR results over 20 minutes with five electrode sizes. It was noted that the electrode performance improvements over time occurred across all electrode sizes and participants. Electrodes with diameters of 15 mm, 20 mm, and 25 mm get an averaged converged SNR of  $28.88 \pm 2.21$  dB,  $29.67 \pm 2.93$  dB, and  $29.63 \pm 4.03$  dB, respectively, which is equal or close to the performance of the standard adhesive gel electrode at  $29.47 \pm 4.77$  dB. Electrodes with diameters of 10 mm and 5 mm showed significantly lower SNR of  $22.10 \pm 5.11$  dB and  $17.10 \pm 4.29$  dB. It should be noted that these SNR results are all based on the QRS complex, the highest wave in the ECG signals. For the 5 mm and 10 mm electrodes, while some participants exhibited clear ECG signals, others did not present an identifiable P or T wave, making the ECG signals unsuitable for diagnostic purposes, although still capable of heart rate monitoring. Considering the performance and the size of the electrode, we chose the electrode with a 15 mm diameter for our later experiments. Figure 13 (b) displays the average signal SNR convergence time, defined as the duration until the SNR stabilizes within a 10% range of the final optimal SNR for the 20-minute session. ECG signal quality may fluctuate or degrade during the experiment, likely caused by electrode movement on the skin due to user motions. The signal typically reconverges; however, signals that did not stabilize during the experiment were excluded from the convergence time analysis. No distinct pattern emerges regarding convergence time relative to electrode size, as most values fall within an eight to twelve-minute range. Additionally, convergence

time may vary depending on individual factors such as hydration, skin moisture level, and rate of insensible water loss.

These results from the dry electrode experiments demonstrate the effectiveness of the skin's natural sweating process in enhancing dry electrode performance. Moreover, the findings provide guidance on selecting electrode sizes for balancing signal quality and aesthetic preference. Participants reported no discomfort from wearing the silicone electrodes, and none of them experienced any skin irritation following the experiments, which further demonstrated the skin-friendliness of the necklace electrode.

## 7 Necklace vs. Ground Truth Evaluation

We evaluate the performance of the ECG Necklace compared to an FDA-approved Holter monitor during controlled activities. The study is designed to evaluate the necklace's performance in real-world conditions with activity labels.

### 7.1 Study Protocol

Given ECG Necklace is aimed to monitor ECG signals during everyday context, we designed a real-world experiment to evaluate the ECG signal's quality and availability during common daily activities, such as using a laptop, chatting, playing phones, and walking. We recruited twelve participants (eight females, four males, average age  $24.1 \pm 2.5$ , average BMI  $21.3 \pm 1.5$ ) for this study. Each participant was asked to wear an ECG necklace with electrodes 15 mm in diameter, as well as an FDA-approved Lepu PC-80B EasyECG holter monitor. Participants were asked to perform various common activities in a large office environment. The environment contains typical electronic interference from over twenty computers, monitors, and the presence of other individuals.

The **study protocol** was structured as follows:

**1) Preparation:** Participants wear the ECG necklace for twenty minutes to prepare the electrodes (as discussed in Section 6.2). During this period, they are free to engage in any activities.

**2) Laptop round 1:** Participants use their own laptops in a natural manner for five minutes.

**3) Chatting round 1:** Participants chat naturally for five minutes, either with the researchers or anyone.

**4) Smartphone round 1:** Participants naturally use their smartphone for five minutes.

**5) Walking:** Participants walk indoors at their normal pace for ten minutes, including walking up and down stairs. This task is guided by researchers, and participants are allowed to rest whenever needed.

**6) Round 2:** Repeat 2), 3), 4) again.

The structure of the study is designed to collect data in real-world conditions with activity labels. In addition, the 10-minute walking session is a common, mild task that promotes the user's natural sweating. We will further compare the ECG signal quality and valid percentage before and after walking.

### 7.2 Valid ECG Percentage

Figure 14 (a) shows the percentage of valid ECG waveforms during each activity. The valid ECG waveform was defined in Section 5. As expected, using laptops, chatting, and using smartphones all yield a high percentage of valid ECG signals.

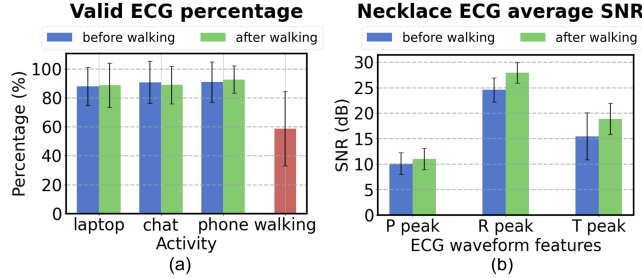


**Figure 14:** (a) The percentage of available valid ECG signal from the necklace during different activities. (b) The average SNR of the P, R, and T peaks in the ECG signals captured by the necklace.

For using laptops, the average available percentage of valid ECG across the twelve users is  $87.96 \pm 13.21\%$  during the laptop round 1 session, and  $88.80 \pm 15.31\%$  during the laptop round 2 session. The highest valid ECG rate was 98.94% (P4), while the lowest was 55.64% (P2). Differences are likely from user activity; stationary tasks like reading or watching videos produced more stable ECG signals than typing, which involves shoulder muscles that can affect the ECG signal from the necklace. For natural chatting, the average available percentage is  $90.76 \pm 14.63\%$  during chatting round 1, and  $88.89 \pm 13.05\%$  during chatting round 2. During using smartphones, the average valid ECG percentage is  $90.92 \pm 13.9\%$  during smartphone round 1, and  $92.65 \pm 9.48\%$  during smartphone round 2, with a maximum percentage up to 100% from P4 and P7.

During walking, even when there were large motions, the average valid ECG percentage during walking was  $58.7 \pm 25.73\%$ , with a high of 95.05% (P8) and a low of 18.36% (P5). Variability likely arose from walking patterns; stable leg-only movements had less impact on the signal, while significant shoulder movement or jumping can disrupt the ECG. This is likely because the shoulder movement can alter skin-electrode contact and introduce additional muscle-generated voltage signals that interfere with the ECG.

Overall, the results show that it is possible to capture valid ECG signals during these common daily activities, but people's behavior can vary. In addition, we do not observe a significant change in valid ECG percentage for sessions before and after walking.

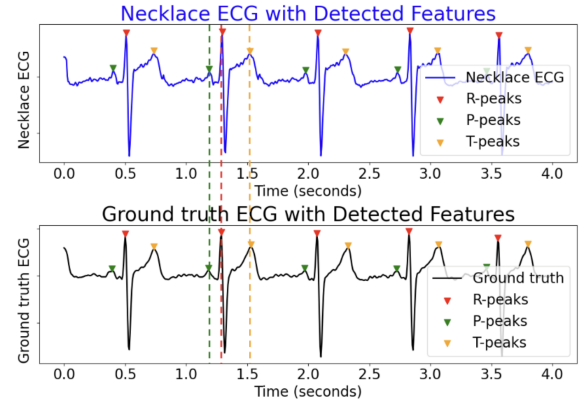
### 7.3 SNR Results

Figure 14 (b) shows the average SNR results of the P peak, R peak, and T peak of the valid ECG identified in Section 7.2 before and after walking. Since the P wave is the smallest wave in ECG, it has the lowest SNR compared to the R peak and T peak but still offers  $10.08 \pm 2.13$  dB from the sessions before walking and  $10.99 \pm 2.26$  dB from the sessions after walking. R peak corresponds to the depolarization of the main mass of the ventricles; hence, it is the largest wave. The average R peak SNR is  $24.5 \pm 2.35$  dB from sessions before walking, and  $27.92 \pm 2.01$  dB from sessions after walking. The T peak corresponds to ventricular repolarization and is an asymmetrical wave with round peak that is usually below R wave but higher than P wave. The average T wave SNR is  $15.48 \pm 4.63$  dB from sessions before walking, and  $18.85 \pm 3.09$  dB after walking.

The ECG signal obtained from the necklace did show a significant SNR improvement after 10 minutes of walking, even though most participants reported they did not feel sweating. This is likely

because of an increased metabolic rate during walking, which triggers the body's thermal regulation even during mild activities. As a result, even without noticeable sweating, the necklace electrode performance was enhanced by the generated skin moisture. This finding indicates that everyday activities like walking could further enhance the performance of the ECG necklace.

### 7.4 ECG timing accuracy



**Figure 15:** An example of synchronized ECG signals obtained from the ECG necklace and the ground truth device, with the P, R, and T waves identified by the NeuroKit2 Python tool.

We compared the ECG Necklace to an FDA-approved Holter monitor by analyzing the timing of detected P, R, and T waves, a key metric for diagnosing cardiac conditions. The necklace ECG signal was resampled from 250 Hz to 150 Hz to match the Holter monitor's sampling rate and then synchronized using cross-correlation. Both signals were processed using the pipeline described in Section 5, and timing errors were calculated by comparing the indices of detected peaks. It is important to note that while the electrodes were placed as closely as possible for simultaneous recording, slight differences in placement introduced minor variations in the ECG signals.

Figure 15 shows an example of the synchronized ECG signals from the necklace and the ground truth device, highlighting the P, R, and T peaks identified by the NeuroKit2 functions. We compared the timing difference of these detected P, R, and T peaks from our necklace ECG and the ground truth ECG. This analysis was restricted to ECG signals that are considered valid only, as discussed in Section 7.2. The average absolute timing error for the P, R, T peak across participants is shown in Figure 16.

The average absolute timing difference of P peak from necklace versus from the ground truth device is only  $8.53 \pm 3.46$  milliseconds, which correspond to 1.3 samples of the ECG data with 150 Hz sampling rate. The average timing difference of R peak is  $3.22 \pm 1.34$  milliseconds, which corresponds to 0.5 samples. The R peak is the sharpest wave in the ECG signals, which makes it easy to identify and less likely to be affected by noise, thus it has the highest alignment accuracy with the ground truth ECG. The average timing difference of T peak is  $15.74 \pm 4.22$  milliseconds, which corresponds to 2.4 samples in the ECG signal. The T wave is usually a more rounded shape peak instead of a sharp peak compared to R wave and P wave, so the T peak is more likely to be identified as an ambiguous

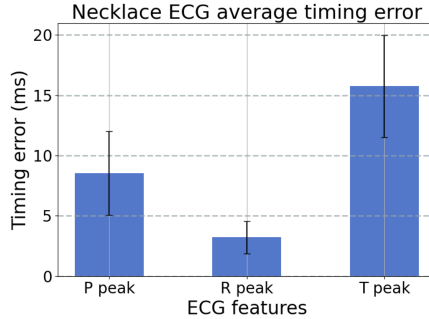


**Figure 16:** The average timing error of P, R, T peaks identified from the necklace ECG versus from the ground truth.

peak by the NeuroKit2 tool. In addition, the T wave duration is typically around 160 to 240 milliseconds, much longer than the P wave and QRS complex. Given that the generally acceptable timing error range for ECG peaks is 20 milliseconds [14], our system demonstrates high accuracy with a well-acceptable error range. In addition, it should also be noted that some of the timing errors may be caused by the detection capabilities of the NeuroKit2 tool, which can introduce errors in identifying the P, R, and T peaks in both the necklace and ground truth ECGs.

## 8 In-the-wild study

We recruited ten participants to wear the ECG Necklace for approximately eight daytime hours during their normal daily routines. The participants included six female, three male, and one non-binary individuals, with an average age of  $24.8 \pm 3.1$  years and an average BMI of  $22.3 \pm 2.1$ . The participants were instructed to wear the ECG Necklace (without the fashion design components) and a Polar H10 chest strap for comparison while continuing their normal daily activities. Although the Polar H10 chest strap is primarily designed for heart rate monitoring with non-standard electrode placement, it was selected for its wearability, continuous ECG sensing, and raw ECG data access. ECG patch monitors are not available for comparison since they require prescriptions and only report analyzed results instead of raw ECG data. Each participant was provided an Android phone with the ECG Necklace app to collect data and an iPhone to record Polar chest strap data. They were told that they could take off any device early if they felt discomfort. At the end of the study, participants were also asked to complete an online survey to rate the comfort of ECG Necklace.

### 8.1 ECG Signal Availability and SNR

Figure 17 (a) shows the percentage of valid ECG signals captured for each participant using the ECG necklace and the Polar chest strap. For P2, the chest strap failed to record any data due to a dead battery, so only the necklace results are presented for this participant. The ECG necklace demonstrated slightly lower but comparable signal availability to the tightly worn chest strap. On average, the necklace captured valid ECG signals  $79.65 \pm 18.3$  % of the time, while the chest strap achieved  $91.69 \pm 5.6$  %. The larger variance in necklace performance stems primarily from P9, which only had 26% valid ECG signals recorded. This discrepancy is likely caused by motion or pose changes, leading to deterioration in the

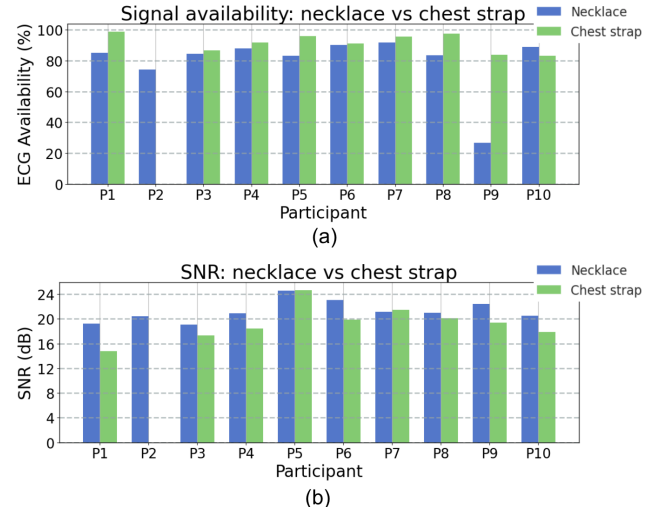


**Figure 17:** (a) The percentage of valid ECG signals by necklace versus by chest strap for each participant. (b) The average SNR results by necklace versus by chest strap for each participant.

electrode's contact with the skin. Additionally, we noticed that P2's signals exhibited a sudden drop in ECG availability from the necklace during the last two hours of the study, likely due to similar motion-induced detachment. Future improvements could involve adding a weighted pendant to the electrodes to enhance resilience to motion. While the chest strap performed well in terms of ECG signal availability, its tightly worn design caused discomfort for several participants, which we will discuss in the later section.

Figure 17 (b) shows the R-peak SNR of the ECG signals recorded by the necklace and chest strap. These SNR values are computed using only the valid ECG signals. The necklace demonstrated higher SNR values for most participants except P5 and P7. On average, the necklace achieved a higher SNR of  $21.23 \pm 1.6$  dB, compared to the chest strap's  $19.33 \pm 2.6$  dB. This result suggests that, despite slightly lower signal availability, the necklace provides better signal quality for the majority of participants. Indeed, we expected these results, as the Polar chest strap is primarily designed for heart rate monitoring during physical activity rather than diagnostic-grade ECG signal acquisition. However, the chest strap remains the closest ECG wearable monitor available on the market for comparison. These results further demonstrate the potential of the ECG Necklace to bridge the gap for daily wearable ECG monitors. These results highlight the ECG Necklace as a promising solution for continuous and accurate use in everyday life.

### 8.2 ECG Necklace Comfort Level

We collected the participant's comfort level with the necklace and the chest strap after wearing each for a whole day. Figure 18 (a) shows the user preference for the necklace versus the chest strap. Most users strongly preferred the necklace over the chest strap for daily wear, with eight users giving a score of 1 or 2, with 1 meaning that they strongly preferred the necklace; one user giving a score of 3, which means that they slightly preferred the necklace; and one user giving a score of 5, indicating that they preferred

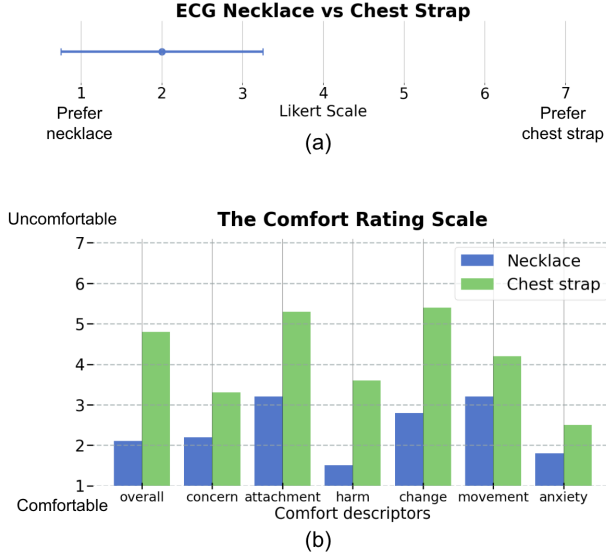


**Figure 18:** (a) The overall comfort level of ECG Necklace and the Polar chest strap. (b) The comfort rating scale results of ECG Necklace and Polar chest strap.

the chest strap. The user who gave a score of 5 indicated that they “felt very aware of the necklace with the fear that it could get disconnected (to the phone)”, and the user was “anxious about potentially disturbing the signal.” However, this user also indicated that “but when everything was working as it should, I thought it was less noticeable”, and “Actually, the silicone stick-on tabs were very comfortable, it felt like a second skin.”

We further analyzed the participant’s comfort level by asking them to rate their comfort levels with each device based on Knight et al.’s comfort rating scales, designed to measure the comfort of wearable devices across 6 dimensions [34]:

- **Concern:** Worries about appearance when wearing the device.
- **Attachment:** Awareness of device presence/movement.
- **Harm:** Feeling that the device may cause harm/pain.
- **Change:** Feeling physically different while wearing the device.
- **Movement:** Device restricting movement.
- **Anxiety:** Insecurity while wearing the device.

The ECG Necklace consistently received lower (indicating more comfortable) scores for overall comfort and across all comfort descriptors, as shown in Figure 18 (b). Specifically, eight out of ten users rated the necklace as overall very comfortable (giving a score of 1 or 2), while only 3 users rated the chest strap as comfortable (one score of 2, and two score of 3). Four participants found the chest strap highly uncomfortable (giving a score of 7 or 6), with some reporting uncomfortable breathing after wearing it for more than an hour. One female participant also mentioned that the chest strap’s placement felt “strange” and “awkward”. In addition, the Necklace was rated significantly more comfortable than the chest strap in the “attachment” and “change” category.

In conclusion, our findings show that ECG Necklace is considerably more comfortable than the chest strap, the most commonly

used device for continuous ECG monitoring. The fact that all participants rated ECG Necklace as comfortable and most participants are willing to wear it every day shows that it is a promising platform for longitudinal health monitoring.

## 9 Discussion

### 9.1 Fashion Design

Fashion considerations are essential when integrating technology into necklaces, as they are primarily designed as fashion accessories. Since the ECG necklace consists of a central processing unit and two electrodes connected by wires, our fashion design focused on decorating these components while maintaining the system’s functionality. Figure 1 shows our example fashion design for the ECG necklace. Inspired by the silver spiral patterns on the electrodes, the design incorporates similar shapes to connect the central pendant with the electrodes seamlessly. The design was 3D-printed, featuring a decorative pendant that conceals the central processing unit and two subtly spiral-shaped covers for the electrodes. To enhance its aesthetic, small pearls were added as decorative elements.

While the showcased design is 3D-printed, alternative designs could incorporate gemstone, pearl, or metal-based pendants paired with chains made from various materials such as metal, leather, or string to achieve a distinct aesthetic. Necklace structural variations, such as positioning the electrodes at the front and back center, are also worth exploring, though they may come with trade-offs in signal quality. Additionally, the electrodes could be redesigned as thin, chain-like elements that seamlessly integrate with the necklace chain, enhancing both functionality and visual appeal.

### 9.2 Necklace as a health monitoring platform

In this work, we primarily explored the ECG sensing capability of the necklace. However, we envision that a smart necklace could serve as a versatile health monitoring platform beyond ECG. Our necklace prototype integrates an accelerometer and a temperature sensor, offering additional functionalities. Positioned directly on the chest, the accelerometer can capture subtle chest movements to detect breathing and heartbeat. Furthermore, measuring skin temperature at the chest can provide a more accurate approximation of core body temperature compared to other wearables, such as smartwatches.

Our initial exploration demonstrated that the accelerometer from the necklace can detect breathing signals and seismocardiography (SCG). However, these capabilities were not extensively evaluated or included in this paper, as they fall outside the primary scope. Future work could explore sensor fusion between ECG and SCG signals, leveraging their timing differences to derive valuable physiological insights. Additionally, the accelerometer could detect moments of user stability to opportunistically trigger ECG sensing, enhancing both energy efficiency and data quality.

### 9.3 Limitation and future work

It is well-known that body hair can significantly degrade the quality of ECG signals, even with standard adhesive electrodes. Our study did not include participants with noticeable body hair around the neck area. Typically, individuals are required to shave and prepare

the skin before a standard ECG test to eliminate air gaps caused by body hair, which can interfere with electrode contact [41].

For future research directions, we aim to assess the clinical utility of the ECG necklace by involving patients with heart conditions. Additionally, we plan to enhance the necklace by integrating advanced algorithms or machine learning models to facilitate computational diagnosis, such as detecting atrial fibrillation (Afib).

## 10 Conclusion

We developed a compact wireless necklace for longitudinal ECG monitoring. Leveraging the unique position and shape of the necklace, the ECG necklace can accommodate two electrodes that are positioned on different sides of the heart, enabling continuous ECG monitoring that other wearables located on the limbs cannot achieve. In addition to the necklace system, we introduced an innovative skin moisture-enhanced electrode that maintains high signal quality without causing skin irritation or suffering performance degradation due to gel evaporation. This electrode utilizes skin-friendly silicone to create a moisturizing micro-environment, leveraging the natural moisture produced by the human body as a conductive "gel". We explored several design aspects of the necklace, including the electrode placement and its size. The results showed that our necklace can provide ECG signals similar to those of a clinical standard Lead I ECG, and our electrode performance is comparable to that of standard adhesive gel electrodes as well. We further performed real-world experiments to evaluate the percentage of valid ECG signals during common daily activities and compared its signal quality to that of an FDA-approved ECG device. The high percentage of valid ECG data and high accuracy compared to an FDA-approved device during these natural activities demonstrate the practicality and effectiveness of our ECG necklace in typical daily settings.

## Acknowledgments

This research was supported in part by the Washington Research Foundation endowment funds, NSF awards 2401177 and 2338736, and the Google Faculty research award. We thank all participants in the studies for their time and effort. Additionally, we thank the reviewers for their insightful feedback and constructive suggestions. Finally, we thank all members of the Ubicomp Lab at the University of Washington and Prof. Vikram Iyer's lab.

## References

- [1] M Akdeniz, S Gabriel, A Licherfeld-Kottner, U Blume-Peytavi, and J Kottner. 2018. Transepidermal water loss in healthy adults: a systematic review and meta-analysis update. *British Journal of Dermatology* 179, 5 (2018), 1049–1055.
- [2] Leonardo Angelini, Maurizio Caon, Stefano Carrino, Luc Bergeron, Nathalie Nyffeler, Mélanie Jean-Mairet, and Elena Mugellini. 2013. Designing a desirable smart bracelet for older adults. In *Proceedings of the 2013 ACM conference on Pervasive and ubiquitous computing adjunct publication*. 425–434.
- [3] Apple. 2023. Apple Watch Healthcare. <https://www.apple.com/healthcare/apple-watch/>. Accessed: 2024-04-20.
- [4] Daniel Ashbrook, Patrick Baudisch, and Sean White. 2011. Nenya: subtle and eyes-free mobile input with a magnetically-tracked finger ring. In *Proceedings of the SIGCHI Conference on Human Factors in Computing Systems*. 2043–2046.
- [5] C Assambo, A Baba, R Dozio, and MJ Burke. 2007. Determination of the parameters of the skin-electrode impedance model for ECG measurement. In *Proceedings of the 6th WSEAS international conference on electronics, hardware, wireless and optical communications*. 90–95.
- [6] BardyDx. 2024. BardyDx Carnation Ambulatory Monitor Specifications. [https://www.bardydx.com/wp-content/uploads/2023/07/DN000697B-BDxCAM\\_SpecSheet.pdf](https://www.bardydx.com/wp-content/uploads/2023/07/DN000697B-BDxCAM_SpecSheet.pdf). Accessed: 2024-11-19.
- [7] Sarnab Bhattacharya, Mohammad Nikbakht, Alec Alden, Philip Tan, Jieting Wang, Taha A Alhalimi, Sangjun Kim, Pulin Wang, Hirofumi Tanaka, Animesh Tandon, et al. 2023. A Chest-Conformable, Wireless Electro-Mechanical E-Tattoo for Measuring Multiple Cardiac Time Intervals. *Advanced Electronic Materials* (2023), 2201284.
- [8] Antonia Bosnjak, Alan Kennedy, Pedro Linares, Maira Borges, James McLaughlin, and Omar J Escalona. 2017. Performance assessment of dry electrodes for wearable long term cardiac rhythm monitoring: Skin-electrode impedance spectroscopy. In *2017 39th Annual International Conference of the IEEE Engineering in Medicine and Biology Society (EMBC)*. IEEE, 1861–1864.
- [9] Yetong Cao, Fan Li, Huijie Chen, Xiaochen Liu, Li Zhang, and Yu Wang. 2022. Guard Your Heart Silently: Continuous Electrocardiogram Waveform Monitoring with Wrist-Worn Motion Sensor. *Proceedings of the ACM on Interactive, Mobile, Wearable and Ubiquitous Technologies* 6, 3 (2022), 1–29.
- [10] CDC. 2024. Heart Disease Facts. <https://www.cdc.gov/heart-disease/data-research/facts-stats/index.html>. Accessed: 2024-11-15.
- [11] Sungwoo Chun, Da Wan Kim, Sangyul Baik, Heon Joon Lee, Jung Heon Lee, Suk Ho Bhang, and Changhyun Pang. 2018. Conductive and stretchable adhesive electronics with miniaturized octopus-like suckers against dry/wet skin for biosignal monitoring. *Advanced Functional Materials* 28, 52 (2018), 1805224.
- [12] Sungwoo Chun, Wonkyeong Son, Da Wan Kim, Jihyun Lee, Hyeongho Min, Hachul Jung, Dahye Kwon, A-Hee Kim, Young-Jin Kim, Sang Kyoo Lim, et al. 2019. Water-resistant and skin-adhesive wearable electronics using graphene fabric sensor with octopus-inspired microsuckers. *ACS applied materials & interfaces* 11, 18 (2019), 16951–16957.
- [13] Edward K Chung. 2013. *Ambulatory electrocardiography: holter monitor electrocardiography*. Springer Science & Business Media.
- [14] Gari D Clifford, Francisco Azuaje, Patrick McSharry, et al. 2006. ECG statistics, noise, artifacts, and missing data. *Advanced methods and tools for ECG data analysis* 6, 1 (2006), 18.
- [15] Cleveland Clinic. 2021. Silent Heart Attack. <https://my.clevelandclinic.org/health/diseases/21630-silent-heart-attack>. Accessed: 2024-04-20.
- [16] Cleveland Clinic. 2024. Heart. <https://my.clevelandclinic.org/health/body/21704-heart>. Accessed: 2024-04-20.
- [17] Nicol A Coull, Anna M West, Simon G Hodder, Patrick Wheeler, and George Havenith. 2021. Body mapping of regional sweat distribution in young and older males. *European journal of applied physiology* 121 (2021), 109–125.
- [18] Harry J Davies, Ghena Hammour, Marek Zylinski, Amir Nassibi, Ljubiša Stanković, and Danilo P Mandic. 2024. The Deep-Match Framework: R-Peak Detection in Ear-ECG. *IEEE Transactions on Biomedical Engineering* (2024).
- [19] Isabel del Agua, Daniele Mantione, Usein Ismailov, Ana Sanchez-Sanchez, Nora Aramburu, George G Malliaras, David Mecerreyres, and Esma Ismailova. 2018. DVS-Crosslinked PEDOT: PSS Free-Standing and Textile Electrodes toward Wearable Health Monitoring. *Advanced Materials Technologies* 3, 10 (2018), 1700322.
- [20] John P DiMarco and John T Philbrick. 1990. Use of ambulatory electrocardiographic (Holter) monitoring. *Annals of internal medicine* 113, 1 (1990), 53–68.
- [21] Luke Eckersley, Lynn Sadler, Emma Parry, Kirsten Finucane, and Thomas L Gentles. 2016. Timing of diagnosis affects mortality in critical congenital heart disease. *Archives of disease in childhood* 101, 6 (2016), 516–520.
- [22] Laura M Ferrari, Sudha Sudha, Sergio Tarantini, Roberto Esposti, Francesco Bolzoni, Paolo Cavallari, Christian Cipriani, Virgilio Mattoli, and Francesco Greco. 2018. Ultraconformable temporary tattoo electrodes for electrophysiology. *Advanced Science* 5, 3 (2018), 1700771.
- [23] FitBit. 2023. Fitbit ECG. <https://www.fitbit.com/global/dk/technology/ecg>. Accessed: 2024-04-20.
- [24] Jutta Fortmann, Vanessa Cobus, Wilko Heuten, and Susanne Boll. 2014. Water-Jewel: design and evaluation of a bracelet to promote a better drinking behaviour. In *Proceedings of the 13th international conference on mobile and ubiquitous multimedia*. 58–67.
- [25] Jutta Fortmann, Erika Root, Susanne Boll, and Wilko Heuten. 2016. Tangible apps bracelet: Designing modular wrist-worn digital jewellery for multiple purposes. In *Proceedings of the 2016 ACM Conference on Designing Interactive Systems*. 841–852.
- [26] Frontier. 2024. Frontier X2 Heart Monitor. <https://fourthfrontier.com/products/frontier-x>. Accessed: 2024-01-29.
- [27] Joule. 2022. Joule Earring Backings. <https://shopjoule.com>. Accessed: 2023-04-20.
- [28] Shideh Kabiri Ameri, Rebecca Ho, Hongwoo Jang, Li Tao, Youhua Wang, Liu Wang, David M Schnyer, Deji Akinwande, and Nanshu Lu. 2017. Graphene electronic tattoo sensors. *ACS nano* 11, 8 (2017), 7634–7641.
- [29] Haik Kalantarian, Nabil Alshurafa, Tuan Le, and Majid Sarrafzadeh. 2015. Non-invasive detection of medication adherence using a digital smart necklace. In *2015 IEEE International Conference on Pervasive Computing and Communication Workshops (PerCom Workshops)*. IEEE, 348–353.
- [30] Kardia. 2023. Apple Watch Healthcare. <https://store.kardia.com/products/kardiamobile>. Accessed: 2024-04-29.

- [31] Kirti Khunti. 2014. Accurate interpretation of the 12-lead ECG electrode placement: A systematic review. *Health Education Journal* 73, 5 (2014), 610–623.
- [32] Hyeonseok Kim, Eugene Kim, ChanYeong Choi, and Woon-Hong Yeo. 2022. Advances in soft and dry electrodes for wearable health monitoring devices. *Micromachines* 13, 4 (2022), 629.
- [33] Taehoon Kim, Junyong Park, Jongmoo Sohn, Donghwi Cho, and Seokwoo Jeon. 2016. Bioinspired, highly stretchable, and conductive dry adhesives based on 1D-2D hybrid carbon nanocomposites for all-in-one ECG electrodes. *ACS nano* 10, 4 (2016), 4770–4778.
- [34] James Knight, Chris Baber, Anthony Schwirtz, and Huw Bristow. 2002. The comfort assessment of wearable computers. *Proceedings. Sixth International Symposium on Wearable Computers* (2002), 65–72.
- [35] Young-Tae Kwon, Yun-Soung Kim, Shinjae Kwon, Musa Mahmood, Hyo-Ryoung Lim, Si-Woo Park, Sung-Oong Kang, Jeongmoon J Choi, Robert Herbert, Young C Jang, et al. 2020. All-printed nanomembrane wireless bioelectronics using a biocompatible solderable graphene for multimodal human-machine interfaces. *Nature communications* 11, 1 (2020), 3450.
- [36] Qingsong Li, Geng Chen, Yajing Cui, Shaobo Ji, Zhiyuan Liu, Changjin Wan, Yiping Liu, Yehu Lu, Changxian Wang, Nan Zhang, et al. 2021. Highly thermal-wet comfortable and conformal silk-based electrodes for on-skin sensors with sweat tolerance. *ACS nano* 15, 6 (2021), 9955–9966.
- [37] Xiaoping Liang, Haifang Li, Jinxin Dou, Qi Wang, Wenya He, Chunya Wang, Donghang Li, Jin-Ming Lin, and Yingying Zhang. 2020. Stable and biocompatible carbon nanotube ink mediated by silk protein for printed electronics. *Advanced Materials* 32, 31 (2020), 2000165.
- [38] Li-Wei Lo, Junyi Zhao, Haochuan Wan, Yong Wang, Shantanu Chakrabarty, and Chuan Wang. 2021. An inkjet-printed PEDOT: PSS-based stretchable conductor for wearable health monitoring device applications. *ACS Applied Materials & Interfaces* 13, 18 (2021), 21693–21702.
- [39] Fei Lu, Chenshuo Wang, Rongjian Zhao, Lidong Du, Zhen Fang, Xiuhua Guo, and Zhan Zhao. 2018. Review of stratum corneum impedance measurement in non-invasive penetration application. *Biosensors* 8, 2 (2018), 31.
- [40] Dominique Makowski, Tam Pham, Zen J. Lau, Jan C. Brammer, François Lépinas, Hung Pham, Christopher Schölzel, and S. H. Annabel Chen. 2021. NeuroKit2: A Python toolbox for neurophysiological signal processing. *Behavior Research Methods* 53, 4 (feb 2021), 1689–1696. <https://doi.org/10.3758/s13428-020-01516-y>
- [41] John Hopkins Medicine. 2024. Electrocardiogram. <https://www.hopkinsmedicine.org/health/treatment-tests-and-therapies/electrocardiogram>. Accessed: 2024-04-25.
- [42] Robert A Nawrocki, Hanbit Jin, Sunghoon Lee, Tomoyuki Yokota, Masaki Sekino, and Takao Someya. 2018. Self-adhesive and ultra-conformable, sub-300 nm dry thin-film electrodes for surface monitoring of biopotentials. *Advanced Functional Materials* 28, 36 (2018), 1803279.
- [43] National Institute of Health. 2024. Subject Preparation: ECG/EKG. [https://megcore.nih.gov/index.php/Subject\\_Preparation:\\_ECG/EKG](https://megcore.nih.gov/index.php/Subject_Preparation:_ECG/EKG). Accessed: 2024-12-09.
- [44] Jaeyeon Park, Hyeon Cho, Rajesh Krishna Balan, and JeongGil Ko. 2020. Heartquake: Accurate low-cost non-invasive ecg monitoring using bed-mounted geophones. *Proceedings of the ACM on Interactive, Mobile, Wearable and Ubiquitous Technologies* 4, 3 (2020), 1–28.
- [45] BardyDx CAM Patch. 2024. BardyDx Carnation Ambulatory Monitor Specifications. <https://www.bardydxdx.com/solutions/cam/>. Accessed: 2024-12-08.
- [46] Julien Penders, Jef van de Molengraft, Marco Altini, Firat Yazicioglu, and Chris Van Hoof. 2011. A low-power wireless ECG necklace for reliable cardiac activity monitoring on-the-move. In *Proceedings of the International Conference of the IEEE Engineering in Medicine and Biology Society*. 1806–1809.
- [47] Ming-Zher Poh, Nicholas C Swenson, and Rosalind W Picard. 2010. Motion-tolerant magnetic earring sensor and wireless earpiece for wearable photoplethysmography. *IEEE Transactions on Information Technology in Biomedicine* 14, 3 (2010), 786–794.
- [48] Polar. 2024. Polar Heart Rate Sensor. <https://www.polar.com/us-en/sensors/h10-heart-rate-sensor>. Accessed: 2024-12-09.
- [49] R Rajaganesan, CL Ludlam, DP Francis, SV Parasramka, and R Sutton. 2008. Accuracy in ECG lead placement among technicians, nurses, general physicians and cardiologists. *International journal of clinical practice* 62, 1 (2008), 65–70.
- [50] Lawrence Rosenthal. 2024. Normal Electrocardiography (ECG) Intervals. <https://emedicine.medscape.com/article/2172196-overview>. Accessed: 2024-04-29.
- [51] Arman Sargolzaei, Karim Faez, and Saman Sargolzaei. 2009. A new robust wavelet based algorithm for baseline wandering cancellation in ECG signals. In *2009 IEEE International Conference on Signal and Image Processing Applications*. IEEE, 33–38.
- [52] Harvard Medical School. 2020. The danger of "silent" heart attack. <https://www.health.harvard.edu/heart-health/the-danger-of-silent-heart-attacks>. Accessed: 2024-04-20.
- [53] Madison S Spach, Roger C Barr, James W Havstad, and E Croft Long. 1966. Skin-electrode impedance and its effect on recording cardiac potentials. *Circulation* 34, 4 (1966), 649–656.
- [54] Takaki Suetake, Shu Sasai, Ya-Xian Zhen, and Hachiro Tagami. 2000. Effects of silicone gel sheet on the stratum corneum hydration. *British journal of plastic surgery* 53, 6 (2000), 503–507.
- [55] Bohan Sun, Richard N McCay, Shivam Goswami, Yadong Xu, Cheng Zhang, Yun Ling, Jian Lin, and Zheng Yan. 2018. Gas-permeable, multifunctional on-skin electronics based on laser-induced porous graphene and sugar-templated elastomer sponges. *Advanced Materials* 30, 50 (2018), 1804327.
- [56] Kenji Suzuki, Taku Hachisu, and Kazuki Iida. 2016. Enhancedtouch: A smart bracelet for enhancing human-human physical touch. In *Proceedings of the 2016 CHI Conference on Human Factors in Computing Systems*. 1282–1293.
- [57] Bahareh Taji, Adrian DC Chan, and Shervin Shirmohammadi. 2018. Effect of pressure on skin-electrode impedance in wearable biomedical measurement devices. *IEEE Transactions on Instrumentation and Measurement* 67, 8 (2018), 1900–1912.
- [58] Bahareh Taji, Shervin Shirmohammadi, and Voicu Groza. 2014. Measuring skin-electrode impedance variation of conductive textile electrodes under pressure. In *2014 IEEE International Instrumentation and Measurement Technology Conference (I2MTC) Proceedings*. IEEE, 1083–1088.
- [59] Vivalink. 2024. Vivalink wearable ECG monitor. <https://www.vivalink.com/wearable-ecg-monitor>. Accessed: 2024-11-19.
- [60] Fan Wang, Xiaoxue Li, Xiuyun Wang, and Xian Jiang. 2020. Efficacy of topical silicone gel in scar management: a systematic review and meta-analysis of randomised controlled trials. *International wound journal* 17, 3 (2020), 765–773.
- [61] Zhi Wang, Beihong Jin, Siheng Li, Fusang Zhang, and Wenbo Zhang. 2023. ECG-grained cardiac monitoring using uwb signals. *Proceedings of the ACM on Interactive, Mobile, Wearable and Ubiquitous Technologies* 6, 4 (2023), 1–25.
- [62] WHO. 2024. Cardiovascular diseases. <https://www.who.int/health-topics/cardiovascular-diseases>. Accessed: 2024-04-25.
- [63] Liping Xie, Zilong Li, Yihan Zhou, Yiliu He, and Jiaxin Zhu. 2020. Computational diagnostic techniques for electrocardiogram signal analysis. *Sensors* 20, 21 (2020), 6318.
- [64] Qiuyue Shirley Xue, Yujia Liu, Joseph Breda, Mastafa Springston, Vikram Iyer, and Shwetak Patel. 2024. Thermal Earring: Low-power Wireless Earring for Longitudinal Earlobe Temperature Sensing. *Proceedings of the ACM on Interactive, Mobile, Wearable and Ubiquitous Technologies* 7, 4 (2024), 1–28.
- [65] Israel Zepeda-Carapia, Agustin Marquez-Espinosa, and Carlos Alvarado-Serrano. 2005. Measurement of skin-electrode impedance for a 12-lead electrocardiogram. In *2005 2nd International Conference on Electrical and Electronics Engineering*. IEEE, 193–195.
- [66] Kang Zhang, Naiwen Kang, Bo Zhang, Ruijie Xie, Jingyu Zhu, Binghua Zou, Yihan Liu, Yuanyuan Chen, Wei Shi, Weina Zhang, et al. 2020. Skin Conformal and Antibacterial PPY-Leather Electrode for ECG Monitoring. *Advanced Electronic Materials* 6, 8 (2020), 2000259.
- [67] Lei Zhang, Kirthika Senthil Kumar, Hao He, Catherine Jiayi Cai, Xu He, Huxin Gao, Shizhong Yue, Changsheng Li, Raymond Chee-Seong Seet, Hongliang Ren, et al. 2020. Fully organic compliant dry electrodes self-adhesive to skin for long-term motion-robust epidermal biopotential monitoring. *Nature communications* 11, 1 (2020), 4683.
- [68] Ruidong Zhang, Mingyang Chen, Benjamin Steeper, Yaxuan Li, Zihan Yan, Yizhuo Chen, Songyun Tao, Tuochao Chen, Hyunchul Lim, and Cheng Zhang. 2021. SpeeChin: a smart necklace for silent speech recognition. *Proceedings of the ACM on Interactive, Mobile, Wearable and Ubiquitous Technologies* 5, 4 (2021), 1–23.
- [69] Zio. 2024. Zio AT Information. <https://fcc.report/FCC-ID/2A9FP-AT18G/3875382.pdf>. Accessed: 2024-11-19.
- [70] Zio. 2024. Zio by iRHYTHM. <https://www.irhythmtech.com/providers/zio-service/zio-monitors>. Accessed: 2024-12-06.
- [71] Oura Health Oy. 2023. Oura Ring. <https://ouraring.com/>. Accessed: 2023-04-12.